

**EEG Delirium Index as a diagnostic screening biomarker in hospitalized nonagenarians: a preliminary validation study**

Supplementary Data

**Table of Appendices**

APPENDIX A: EEG preprocessing pipeline and computation of spectral and variability metrics..... 2  
APPENDIX B: Statistical modeling ..... 4  
APPENDIX C: EEG spectral power and variability..... 5  
REFERENCES..... 6

---

**APPENDIX A: EEG recording, preprocessing, and spectral analysis**

---

This Appendix details the methodology by which EEG recordings were conducted, by which EEG segments were prepared for quantitative analysis, and details the spectral and complexity metrics that were computed for each segment.

Continuous EEG recordings were obtained at the bedside in the ICU according to standard guidelines set forth by the American Clinical Neurophysiology Society (ACNS).<sup>1</sup> Briefly, 19 silver chloride electrodes were affixed to the participant's scalp using conductive paste according to the International 10-20 System of electrode placement. Reference electrode was typically placed at the CPz location, or at the AFz location if the former was infeasible (e.g. due to scalp wound). EEG signals were sampled at 256Hz by a Natus® NeuroWorks data acquisition system and stored on a Windows server. Contiguous, two-minute, seizure-free segments of EEG were clipped, exported to European Data Format (EDF) and de-identified using edf-anonymize.<sup>2</sup> We used 2-minute segments instead of the previously published 5-minute segments, to maximize the number of artifact-free EEG recordings for inclusion while retaining information about the variability of each participant's EEG spectral profile over time. Our institution's standard clinical protocol involves stimulation by the technician (standard orientation questions, eyes opening and closing; in unresponsive patients, passive eye opening and closing, and nailbed pressure) immediately after the EEG recording begins; we selected the period after technician stimulation to target EEG segments when each participant would have been at their most alert, to minimize spurious findings due to changes in EEG frequency composition associated with somnolence or sleep. No stimulus delivery devices were used.

**EEG Preprocessing**

Preprocessing steps were performed using EEGLAB,<sup>3</sup> an open-source, MATLAB®-based toolkit for automated processing and analysis of multichannel stochastic signals. Each deidentified two-minute EEG clip (one per participant) was detrended and bandpass filtered to between 0.5Hz and 50Hz using a 1620-order finite impulse response filter. We conducted automated artifact rejection by a series of processes using the default parameters of the `clean_rawdata` plugin<sup>4</sup> as follows: Isoelectric or noisy channels were removed if they exceeded 4 standard deviations from the mean signal amplitude. Channels whose voltage timecourses have correlation coefficients less than 0.8 with respect to their expected values based on reconstruction from the total channel population were also removed. Artifact-laden segments of time were also identified using the Artifact Subspace Reconstruction (ASR) algorithm.<sup>5</sup> Periods of data wherein greater than 25% of the channels exceeded 7 standard deviations from the norm were also excluded.

After raw EEG data were cleaned, EEG segments were decomposed using the logistic information maximization independent components analysis (ICA) algorithm<sup>6</sup> as implemented by the `runica.m` function in EEGLAB. We used an automated pattern recognition algorithm<sup>7</sup> to detect and exclude components that had 90% or greater probability of representing muscle, electrocardiographic, ocular, or channel noise artifacts, based on a published database of over 200,000 EEG Independent Components.<sup>7</sup> Components were discarded if the probability of their signal representing line noise or channel noise was greater than or equal to 0.8, or if the probability of their signal representing myogenic, ocular or cardiac noise was greater than or equal to 0.9.

After ICA-based extraction, we re-referenced the remaining EEG channels to a common average reference and subdivided recordings into 3-second, nonoverlapping epochs for spectral and complexity analysis. Of the remaining 69 two-minute clips submitted for preprocessing, one clip was discarded due to too few clean epochs remaining after artifact removal to reliably determine representative spectral and complexity characteristics. Of the remaining clips, a total of 57.8% of data signals remained after artifact removal.

**Global Power Spectra and Spectral Variability Metrics**

Using Chronux,<sup>8</sup> a MATLAB®-based signal processing toolbox, and a series of bespoke MATLAB® functions, we computed spectral band power in 5 canonical frequency ranges of interest: delta (1-4Hz), theta (4-8Hz), alpha (8-13Hz), low beta (13-25Hz) and high beta (25-40Hz). For each 3-second epoch, band power estimates were computed individually for each channel. The individual band power was divided by the broadband (1-40Hz) power to yield the relative band power for each channel and epoch. Relative band power was then averaged over all channels globally, and averaged across all 3-second epochs of each preprocessed EEG clip, to yield a single relative power value per frequency band, for each EEG clip. We also computed spectral variability (operationalized as the coefficient of variation, i.e. the mean divided by the standard deviation, of the spectral power within each frequency band of interest) across all 3-second epochs within the 2-minute clips. Resulting

distributions of the relative band power and spectral variability measures are displayed in **Figure S1**. These values were used as input to the following previously published<sup>9</sup> formula for the EEG Delirium Index:

$$\text{EEG-DI} = \log_{10}((15.7 * \text{delta variability}) + (1.1 * \text{high-beta variability}) + (0.7 * \text{relative theta power}) + (1.5 * \text{relative alpha power}))$$

Power spectra were computed according to the Thomson multitaper method<sup>10</sup> using the Chronux function `mtspectrumc` with 5 tapers and a time-bandwidth product of 3.

---

**APPENDIX B: Statistical modeling**

---

Complete case analysis is used for all of the analyses in this report.

Sample Size Analysis

Based on a preliminary screen of our EEG database encompassing May 2014 to January 2020, we estimated a total sample size of 81 participants. We anticipated that we would be able to include independent variables in a logistic regression model with 5 to 8 degrees of freedom (m/10 to m/15 observations per model parameter, where m=81) without overfitting this model.

Logistic Regression

Multivariable Logistic regression modeling was used to determine the association of delirium or coma (modeled as a single composite outcome) with the EEG delirium indicator (EEG-DI) and history of dementia, adjusting for age, sex, and presence of sedation. Logistic regression models use the following form:

$$\log(p(\mathbf{x})/(1-p(\mathbf{x}))) = \beta_0 + \beta_1 \mathbf{x}$$

The effect sizes, 95% confidence intervals, and p-values are reported.

Receiver Operating Characteristic (ROC) Curves

ROC curves were used to determine the ability of the model and the EEG brain state indicator to discriminate between the presence or absence of delirium or coma by showing the trade-off between sensitivity and specificity. These were shown for the full dataset (n=74), and separately for those with (n=23) and without (n=51) a history of dementia. The area under the receiver operating curve (AUC) is reported on the curves.

Internal Validation

Internal validation via bootstrapping was used to measure the predictive accuracy of the model and the EEG brain state indicator on the composite outcome of delirium or coma. In particular, we obtained a measure of the optimism-corrected AUCs and their corresponding 95% CI.

The following steps were performed to obtain optimism correct estimates based on bootstrap resampling:

1. Estimate model performance in the original sample of size n
2. Draw a bootstrap sample of the same size n and fit the model to the bootstrap sample
3. Apply the model obtained in the bootstrap sample to the original sample
4. Subtract the accuracy measure found in the bootstrap sample from the accuracy measure in the original sample - this is the estimate of optimism (i.e. overfitting)
5. Repeat the process 250\* times and average over the repeats to obtain a final estimate of optimism for each measure
6. Subtract that value from the observed/apparent accuracy measure to determine the optimism corrected estimate

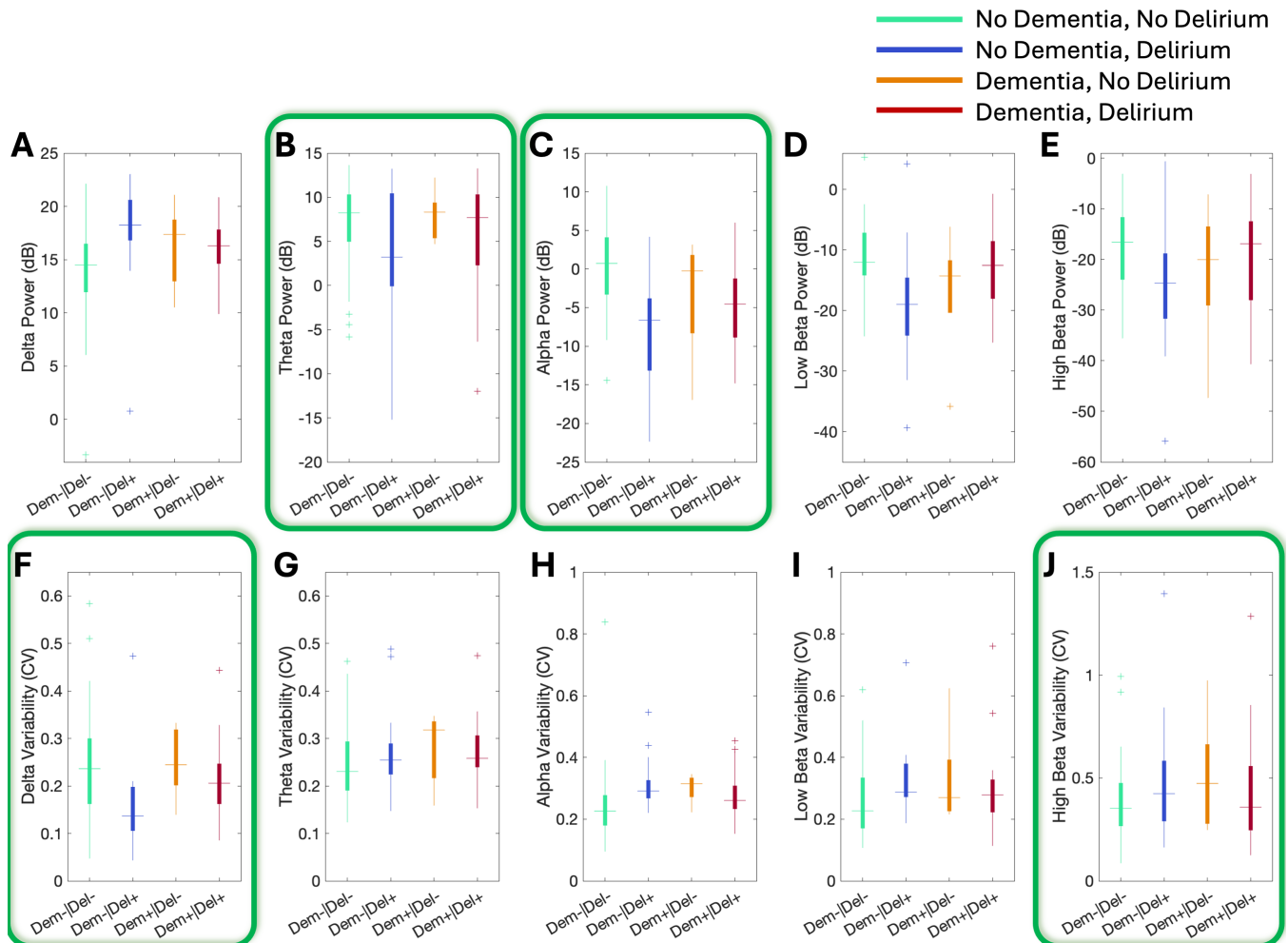
This process was performed separately for the full dataset, for the subset with dementia and for the subset without dementia.

\*When performed on the subset with dementia, a divergence or singularity occurred in 4 samples, leaving 246 repetitions that were used to compute the optimism-corrected AUC in this subgroup.

**APPENDIX C: EEG spectral power and variability**

**Supplementary Figure S1:**

Distributions of spectral power (A-E) and variability (F-J) in 5 canonical frequency bands, by history of dementia and presence/absence of delirium. Spectral variability metrics computed as coefficient of variation (mean divided by standard deviation) of power in the corresponding frequency band across 3-second epochs within each 2-minute clip. A,F: Relative delta (1-4Hz) power and spectral variability; B,G: Relative theta (4-8Hz) power and variability; C,H: Relative alpha (8-15Hz) power and variability; D,I: Relative low-beta (15-25Hz) power and variability; E,J: Relative high-beta (25-40Hz) power and variability. Thick bars represent 25<sup>th</sup>-75<sup>th</sup> percentiles, whiskers represent minimal and maximal values not considered outliers, and + indicate outliers (defined as observations greater than  $q_3 + 1.5 \times (q_3 - q_1)$  or less than  $q_1 - 1.5 \times (q_3 - q_1)$ , where  $q_1$  and  $q_3$  are first and 3<sup>rd</sup> quartiles, respectively). Light green and blue bars represent participants without dementia, without (n=31) and with (n=15) delirium, respectively. Orange and red bars represent participants with dementia, without (n=5) and with (n=17) delirium, respectively. Participants with delirium or dementia tended to have higher relative delta power and lower relative alpha power, consistent with prior literature. Those with delirium tended to have lower delta variability. Plots circled in green indicate metrics required to compute EEG-DI. *dB: Decibel; Del: Delirium; Dem: Dementia.*



---

**REFERENCES**

---

1. Sinha SR, Sullivan L, Sabau D, et al. American Clinical Neurophysiology Society Guideline 1: Minimum Technical Requirements for Performing Clinical Electroencephalography. *J Clin Neurophysiol* 2016; **33**(4): 303–7.
2. Goldberger AL, Amaral LA, Glass L, et al. PhysioBank, PhysioToolkit, and PhysioNet: components of a new research resource for complex physiologic signals. *Circulation* 2000; **101**(23): E215–20.
3. Delorme A, Makeig S. EEGLAB: an open source toolbox for analysis of single-trial EEG dynamics including independent component analysis. *J Neurosci Methods* 2004; **134**(1): 9–21.
4. Kothe C, Miyakoshi M, Delorme A. *clean\_rawdata* (Version 2.6). 2019.
5. Mullen TR, Kothe CA, Chi YM, et al. Real-Time Neuroimaging and Cognitive Monitoring Using Wearable Dry EEG. *IEEE Trans Biomed Eng* 2015; **62**(11): 2553–67.
6. Bell AJ, Sejnowski TJ. An information-maximization approach to blind separation and blind deconvolution. *Neural Comput* 1995; **7**(6): 1129–59.
7. Pion-Tonachini L, Kreutz-Delgado K, Makeig S. ICLLabel: An automated electroencephalographic independent component classifier, dataset, and website. *Neuroimage* 2019; **198**: 181–97.
8. Bokil H, Andrews P, Kulkarni JE, Mehta S, Mitra PP. Chronux: a platform for analyzing neural signals. *J Neurosci Methods* 2010; **192**(1): 146–51.
9. Williams Roberson S, Azeez NA, Fulton JN, et al. Quantitative EEG signatures of delirium and coma in mechanically ventilated ICU patients. *Clin Neurophysiol* 2023; **146**: 40–8.
10. Thomson DJ. Spectrum Estimation and Harmonic-Analysis. *P Ieee* 1982; **70**(9): 1055–96.